INTERNATIONAL JOURNAL OF OPTIMIZATION IN CIVIL ENGINEERING
Int. J. Optim. Civil Eng., 2013; 3(1):179-207

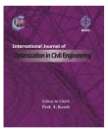

HYBRID ARTIFICIAL NEURAL NETWORKS BASED ON ACO-RPROP FOR GENERATING MULTIPLE SPECTRUM-COMPATIBLE ARTIFICIAL EARTHQUAKE RECORDS FOR SPECIFIED SITE GEOLOGY

G. Ghodrati Amiri [*, †] and P. Namiranian
Center of Excellence for Fundamental Studies in Structural Engineering, School of Civil Engineering, Iran University of Science & Technology, Tehran, IRAN

ABSTRACT

The main objective of this paper is to use ant optimized neural networks to generate artificial earthquake records. In this regard, training accelerograms selected according to the site geology of recorder station and Wavelet Packet Transform (WPT) used to decompose these records. Then Artificial Neural Networks (ANN) optimized with Ant Colony Optimization and resilient Backpropagation algorithm and learn to relate the dimension reduced response spectrum of records to their wavelet packet coefficients. Trained ANNs are capable to produce wavelet packet coefficients for a specified spectrum, so by using inverse WPT artificial accelerograms obtained. By using these tools, the learning time of ANNs reduced salient and generated accelerograms had more spectrum-compatibility and save their essence as earthquake accelerograms.

Received: 27 April 2012; Accepted: 15 January 2013

KEY WORDS: artificial earthquake accelerograms; ant colony optimization algorithm; wavelet packet transform; artificial neural network; principal component analysis; resilient backpropagation algorithm

1. INTRODUCTION

Civil engineers use ‘response spectrum’ to evaluate the seismic response of ordinary

[*]Corresponding author: G. Ghodrati Amiri, Center of Excellence for Fundamental Studies in Structural Engineering, School of Civil Engineering, Iran University of Science & Technology, Tehran, IRAN
[†]E-mail address: ghodrati@iust.ac.ir (Gholamreza Ghodrati Amiri)

structures and to design or seismic rehabilitation of structures to withstand earthquake forces. However, response spectrum process has limitations to provide temporal information on structural response and behavior. Furthermore, major and important structures like dams, power plants and high-rise buildings, need an economical and safe design. For satisfying the criteria of efficient design, engineers should use new design procedures. Time-history analysis, performance based design and controlling of structures are some of these procedures that use earthquake accelerograms. However, there are not enough and appropriate earthquake records in some parts of the world. So generation of artificial earthquake accelerograms that are compatible with a specified spectrum discover an important aspect.

There are many methods for generating spectrum-compatible artificial earthquake accelerograms, which categorized as three or four major fields:

- Stochastic Methods
- Ray-Theory Methods
- Hybrid Method
- New Biologically Soft Computing Methods

Because the method that proposed in this paper is located in the last categorize, just a brief history and major works of this method are demonstrated. New biologically soft computing methods introduced at the recent years with the usage of artificial intelligence for solving inverse problems. Ghaboussi and Lin [1]used a replicator artificial neural network (ANN) for compressing Fourier transform of training accelerograms and then a multi-layer feed-forward (MLFF) was trained to relate the pseudo-velocity response spectrum (PSV) of training set to compressed Fourier transform. With these two ANNs, they could create only a single accelerogram. Then they modified their MLFF by applying Gaussian noise to the outputs of each layer, so this ANN was capable of generating multiple spectrum compatible accelerograms [2]. Lee and Han used five ANNs for this purpose and made relations between seismological parameters and their accelerograms characteristics and response spectrums [3]. Rajasekaran et al. introduced a new method based on Lee and Han algorithm and the ability of Principal Component Analysis (PCA) in dimension reduction of data [4].

Ghodrati Amiri et al. used the abilities of radial basis function (RBF) neural networks and discrete wavelet transform (DWT) to produce a single accelerogram [5]. Next, Ghodrati Amiri et al. used stochastic neural networks to make a relation between PSV and the Wavelet Packet Coefficients (WPC) to generate multiple earthquake accelerograms [6]. Recently, Ghodrati et al. by means of a hybrid GA-MLFF network produced an inverse mapping from a response spectrum to effective principal components of accelerograms' WPC [7].

In this paper, the capability of ANN in solving inverse problems used to generate multiple spectrum-compatible earthquake records for specified site geology. In this regard, some training accelerograms from Iranian strong motion database selected and categorized into Soil and Rock groups according to the site geology of recorder station. ANNs used to make relations between pseudo-velocity or acceleration response spectrums (PSV/PSA) and WPC of training sets. Because response spectrums calculated at 1000 points, for decreasing the number of neurons at input layers of ANNs, we used PCA to select only effective coefficients at response spectrums. Furthermore, for overcoming the drawbacks that encourage at training phase of ANN (rapid convergence on the local optima and long time of

evolving), Ant Colony Optimization algorithm (ACO) combined with resilient backpropagation algorithm are used for evolving ANNs.

2. ANT COLONY OPTIMIZATION ALGORITHM

The initial ant colony algorithm was proposed by Dorigo in order to find a solution for Traveling Salesman Problem (TSP), and was inspired from the real ants' [8]. Ants are social insects that live in big colonies, and one of the very interesting aspects of the behavior of ant species is their ability to find shortest paths between the ants' nest and the food sources. In this operation, when ants leave their nest to find food, they lay down pheromone trails, which other ants then tend to follow it.

The basic ingredient of ACO is the use of a probabilistic solution construction mechanism based on stigmergy. Artificial ants have internal memories, which used for storing the path followed by the ants, and deposit and update pheromone trails so other ants can follow their path according to these amounts. The original algorithm of the ACO can be outlined as algorithm 1.

Algorithm 1: The basic ACO algorithm flow chart [9]

```
Parameter Initialization
Represent the problem by a weighted connect graph
While termination conditions not met do
Ant Solution Construct()
Construct ants' solution according to the amount of pheromone trail matrix
Pheromone Update()
Compute each ant's solution cost and update the pheromone trail matrix
```

The probability of the *k*th ant making the transition from node *i* to node *j* is given by:

$$p_{ij}^{k}(t)=\begin{cases}\dfrac{\left[\tau_{ij}(t)\right]^{\alpha}.\left[\eta_{ij}\right]^{\beta}}{\sum_{k\in allowed_k}\left[\tau_{ij}(t)\right]^{\alpha}.\left[\eta_{ij}\right]^{\beta}} & if\ \ j\in allowed_{k}\\ 0 & otherwise,\end{cases} \tag{1}$$

where $allowed_k$ are the nodes that ants can select them according to given rules and α and β respectively control the relative importance of the pheromone trail and visibility. $\tau_{ij}(t)$ is the pheromone intensity of the path between node *i* and *j* and η_{ij} is the heuristic information and is defined as the quantity $1/d_{ij}$.

After each epoch, the pheromone intensity trails updated according to the following formula:

$$\tau_{ij}(t+n)=(1-\rho).\tau_{ij}(t)+\sum_{k=1}^{N}\Delta\tau_{ij}^{k}, \tag{2}$$

where $\rho \in (0,1]$ is the evaporation rate and $\Delta\tau_{ij}^{k}$ is the quantity of pheromone released on path *(i, j)* by the *k*th ant between time *t* and *t* + *n*, and is calculated by:

$$\Delta\tau_{ij}^{k} = \begin{cases} Q/L_k & \text{if ant } k \text{ used edge } (i,j) \text{ in its tour} \\ 0 & \text{otherwise,} \end{cases} \tag{3}$$

where Q is a constant and L_k is the tour length of the *k*th ant[10].

ACO successfully applied to many numerous combinatorial optimization problems such as TSP, quadratic assignment problems, scheduling problems, and vehicle routing problems [11].

3. ARTIFICIAL NEURAL NETWORKS

Artificial neural networks are a portion of "Expert Systems" or "Computational Intelligence Systems" that inspired from the architecture and internal features of the human brain and nervous system. ANNs are consisting of a large number of simple processing elements called as neurons. Their power comes from the parallel processing of the data's information that follows from input layer to output layer via neurons' connections.

The Multi-layer feed forward (MLFF) neural network is the most common neural network structure. The relationship between the *i*th output (y_i) and the inputs ($x_1,x_2,...,x_p$) has the following mathematical representation [12,13]:

$$y_i = h\left[\sum_{j=1}^{q} w_j . g\left(\sum_{i=1}^{p} w_{ij} . x_i + w_{0ij}\right) + w_{0j}\right], \tag{4}$$

where, *h* and *g* are activation functions of hidden and output layers respectively; w_{ij} (i=0,1,2,…,p, j=1,2,….q) and w_j (j=0,1,2,….q) are connection weights of network; *p* and *q* are the number of nodes at input and hidden layers respectively and w_{0j} and w_{0ij} are biases value of output and hidden layers, respectively.

Back propagation (BP) algorithms are the most popular algorithms that used for training ANNs due to their success from both simplicity and applicability viewpoint. In this regard, the error between the target and output values passed to each unit in the backward direction, and the new modified weight matrix computed in order to minimize the sum-squared error function:

$$E(w_{ij}^{(n)}) = \frac{1}{2}\sum_{p}\sum_{j}\left(t\arg_j^p - out_j^{(N)}(in_i^P)\right)^2 = \frac{1}{2}\sum_{p}\sum_{j} e_j^2 \tag{5}$$

Modification process contains a series of gradient descent weight updates as follow:

$$w_{ij}^{k}(t+1) = w_{ij}^{k}(t) + \eta.\delta_{ij}^{k}.y_{m(j-1)i} \tag{6}$$

$$\begin{cases} \delta_{mj}^{k} = f'(z_{mj}^{k}).\sum_{i=1}^{N_{j+1}} \delta_{m(j+1)i}.w_{(j+1)i}^{k}(t) \;\; j = L-1,...,1, \\ \delta_{mj}^{k} = f'(z_{mj}^{k}).e_{mj}^{k}, \end{cases} \tag{7}$$

where, z_{mj}^{k} is the input of each neuron that is the weighted sum of the outputs from the previous layer; *t* is the number of training set; *L+1* is the number of layers in the network; *f ′(*)* is the derivative of the activation function, η is a positive constant, called learning factor [14].

BP algorithms consist of several training methods such as Quasi-Newton algorithms, Levenberg-Marquardt method, Conjugate Gradient algorithms, Resilient Backpropagation algorithm, etc. All of these algorithms have their benefits and suitable for specified ANNs according to the number of layers, nodes and transfer functions in each layer. Because we use squashing functions in our ANNs and the number of weights in the networks is too large, we use Resilient Backpropagation algorithm to eliminate harmful effects of squashing functions in the magnitudes of the partial derivatives and for faster training.

4. WAVELET PACKET TRANSFORM

The first transform that used for analyzing earthquake accelerograms was Fourier Transform, which obtained the frequency contents of signals over the analysis window and, as such, lacks any time domain localization information. Wavelet Transform (WT) uses long time windows to get a finer low-frequency resolution and short time windows to get high-frequency information of signals. Thus, WT gives precise frequency information at low frequencies and precise time information at high frequencies [15]. In Discrete Wavelet Transform (DWT), we downsample the original signal into two groups of coefficients: Approximations (cA) and Details (cD), which contain low-frequency components and high-frequency components of signal, respectively. The decomposition process can be iterated, by applying this procedure to the cA of the upper level so signal is broken down into many lower-resolution components.

The Wavelet Packet Transform (WPT) is an important extension of the DWT, which performs decomposition on both the Approximations and the Details. Therefore, in the WP decomposition of a signal, the signal is filtered with both low-pass (LP) and high-pass (HP) filters named as quadratic mirror filters.

Wavelet packets ($\omega_{j,m}^{k}(t)$) are a collection of basis function $2^{-j/2}\omega_{m}(2^{-j}t-k)$. *j* and *k* are respectively the scaling (frequency localization) parameter and the translation (time localization) parameter, and *m = 0; 1;* ... is the oscillation parameter. The first two wavelet packet functions *(m = 0,1; j = k = 0)* are also called the scaling function $\varphi(t)$ and the mother wavelet $\psi(t)$ [16]:

$$\begin{aligned}\omega_0(t) &= \varphi(t),\\ \omega_1(t) &= \psi(t),\end{aligned} \tag{8}$$

Other wavelet packet functions (m = 2, 3, ...) are defined through the following sequence of functions [17]:

$$\begin{aligned}\omega_{2n}(t) &= \sqrt{2}\sum_l h_l \omega_n(2t-l)\\ \omega_{2n+1}(t) &= \sqrt{2}\sum_l g_l \omega_n(2t-l),\end{aligned} \tag{9}$$

where h_l is the low-pass (scaling) filter and g_l is the high-pass (wavelet) filter.

For a discrete signal, the decomposition coefficients of wavelet packets computed by the following equations:

$$\begin{aligned}x^k_{2n,j+1} &= \sum_l h_{l-2k} x^l_{n,j}\\ x^k_{2n+1,j+1} &= \sum_l g_{l-2k} x^l_{n,j}\end{aligned} \tag{10}$$

The original signal reconstructed iteratively by

$$x^l_{n,j} = \sum_k h_{l-2k} x^k_{2n,j+1} + \sum_l g_{l-2k} x^k_{2n+1,j+1} \tag{11}$$

Figure 1 shows a 2-level WPT based on the Conventional (decimated) DWT.

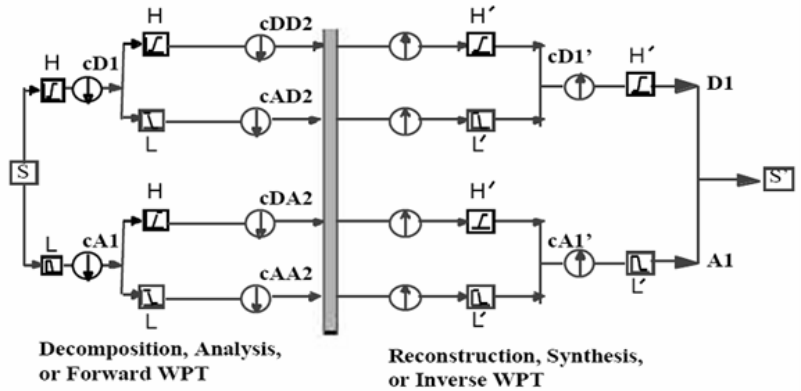

Figure 1. A 2-1evel Wavelet Packet Transform decomposition and reconstruction [34].

5. PRINCIPAL COMPONENT ANALYSIS

The main idea of Principal Component Analysis (PCA) is to reduce dimensionality a data

set that consist of a large number of interrelated variables, while retaining as much as possible of the variation present in the data set. This is achieved by transforing data to a new set of variables, the Principal Components (PCs), which are uncorrelated and are ordered so that the first *few* retain most of the variation present in *all* of the original variables [18].

The main results of PCA are scores, which related to the samples and factor loadings which reflect how much a variable contributes to that particular PC and how well one variable is similar with others. Therefore the higher loading of a variable, the more contribution of variable to the variation that accounted for by the particular PC [19, 20].

Assume that input data X = [X_1 X_2 … Xp] be an $n \times p$ matrix of n observations on p variables and conventionally be columnwise standardized. By using PCA, we postulate that X approximated by the following bilinear structure:

$$\hat{X} = S\,Q^T \tag{12}$$

where S = [S_1 S_2 … S_r] is a $n \times r$ matrix of n component scores on r ($1 \le r \le p$) components, and Q = [Q_1 Q_2 … Q_r] is a $p \times r$ matrix consisting of the eigenvectors of $X^TX/n=I$ and $Q^TQ= D$. Next, we find model parameters S and Q such that

$$\theta = tr(X - \hat{X})^T (X - \hat{X}) \tag{13}$$

is minimized for the prescribed r components [21]. r components can be selected by comparing the total variance of PCs and a desired effective variance ratio (R_{eff}^{var}):

$$\frac{\sum Var_{eff-PC}}{\sum Var_{tot-PC}} \le R_{eff}^{\text{var}} \tag{14}$$

6. THE PROPOSED METHOD

The main objective of this paper is to develop a methodology base on ACO-Rprop for training neural networks that are capable of generating multiple accelerograms for specified input response spectrum that includes the site geology specifications of a specified site. The generated accelerograms should have response spectrums closely approximate to the input response spectrum. In addition, the other characteristics of the generated accelerograms, such as their duration, should be similar to those of the recorded accelerograms used to train the neural networks. This procedure contains three main stages: Data Preparation phase, ANN Training and Testing phase, Artificial Earthquake Records Generation stage.

6.1. Data Preparation phase

The main tool that used for generating accelerograms is ANN that can solve our inverse problem. The inputs of ANNs are the response spectrum of accelerogram and the outputs are the WPCs at level j of the WPT of the earthquake records. Therefore, for generation of multiple spectrum compatible artificial earthquake records, we need a set of historical

accelerograms that used for training ANNs.

Many factors influenced earthquake ground motions, which one of the most important factors is local soil conditions. Soil conditions influence ground motion and its attenuation. Studies on the influence of site geology on ground motion use the average shear wave velocity to identify the soil category. The scrutinizes show that for the same distance, magnitude, and fault mechanism, as the soil becomes stiffer (i.e. a higher shear wave velocity), the peak ground acceleration becomes smaller. In addition, there is a general agreement between various investigators that the soil condition has a pronounced influence on velocity and displacement of earthquake, and accelerograms that recorded on soil subsoil have larger peak horizontal velocity than those recorded on rock subsoil [22].

This factor was not entered in the models of previous related works. In this study, we will apply this factor by categorizing the training accelerograms into two groups: Rock & Soil, according to the site geology of their recorder stations. Because we use Iranian strong motion, we use Iranian seismic design code (Standard No.2800-05 3rd Edition) in this classification. Table 1 shows this standard criterion for site geology categorizing:

Table 1: Site Geology according to Iranian seismic design code

Ground Type	**Explanation of materials**	**Shear wave velocity (m/s)**
I	Un-weathered igneous rocks, hard sedimentary rocks and metamorphic rocks (as gneisses and crystalline silicate rocks) Very hard conglomerates very compact and very hard sediment	$V_S>750$ $375<V_S<750$
II	Soft igneous rocks e.g. tuffs, clay stones, shale and semi-weathered or altered rocks Crushed (but not hardly) hard rocks , foliated metamorphic rocks, conglomerate and compact sand and gravel	$375<V_S<750$
III	Weathered rocks, semi-compact sands and gravels, other compact sediments Compact sandy clay soils, with low ground water level	$175<V_S<375$
IV	Soft sediments, clay soils, weak cemented and un-cemented sands, incompact soils with high ground water level Any kind of soft soils	$V_S<175$

According to this table, soil types I & II are Rock $(375 \le V_S)$ and soil types III & IV are Soil $(375 > V_S)$ and grouping training set is accomplished according to the average shear wave velocity for the upper 30 meters of the soil layer under the stations that record accelerograms.

The peak ground acceleration (PGA) of all the accelerograms scaled to *1g* so we could compare their response spectrum. Next, we categorize accelerograms in four duration groups 10, 20, 30, and 40 seconds, based on their bracketed durations (0.05g as acceleartaion level). For better and faster training of ANNs, PGA of all accelerograms in each group shifted to make the PGA of each accelerogram aligned at the same time. This operation is performing by adding or deleting zeros from the start or end of accelerograms in specified manner so

navigates of them not changed. Tables 2 to 8 show the list of earthquake records, used in training set of the ANNs, in each soil condition and duration group.

It should be noted that for the group of 10 sec duration and Soil site geology, researchers could not find any suitable records for training ANNs.

Table 2: List of training earthquake records, 10 sec duration, Site geology: Rock [31]

Earthquake	Station	Date	Magnitude M_S	Modified PGA (cm/sec^2)	Duration (sec)
NAGHAN	NAGHAN	1977.04.06	6.2	761	9
	TABAS	1978.09.17	4.8	93.5	8.34
	SHALAMZAR	1984.06.01	5	337.2	8.4
	SARI	1990.01.20	5.8	143.1	9.2
	HOSSEINEH OLYA	1994.07.31	5	180.5	7.6
	SADABAD	1996.01.24	4.6	32.8	8.4
	KARIQ	1997.03.02	5	264.3	7.6
	HAMEDAN	1998.08.24	4.5	27.6	8.3
	NAHAVAND	1998.08.25	4.5	84	7.9
	DAM(HINY MINY)	1998.10.04	4.8	359	6
	CHENAR	1998.10.04	4.8	20.1	9.6
	KHONJ	1998.11.13	5.1	397.3	9.6
	AHRAM	1999.09.24	4.7	143.2	9
	AHRAM	1999.09.25	4.6	38.4	9.74
	AHRAM	1999.09.25	4.6	15.5	9.84
	Faryab	2000.03.11	4.3	23.9	9
	Tange Eram	2001.05.06	4.2	38.2	9
	Borazjan	2001.05.07	4.2	27.6	8.1
	Roodbar	2001.08.20	4.1	27.9	6.4
	Bandar-e-Asaluyeh	2002.02.27	4.2	48.6	6.9
	Tange Eram	2002.06.23	4	65.9	7.4
	Sirch	2003.04.16	4.2	75.2	8

Table 3: List of training earthquake records, 20 sec duration, Site geology: Rock [31]

Earthquake	Station	Date	Magnitude M_S	Modified PGA (cm/sec^2)	Duration (sec)
	SIRCH	1989.11.20	5.7	65	18.3
	ZARRAT	1994.06.18	5	111.5	18
	ZANJIRAN	1994.06.18	5	87.8	18
ZANJIRAN	ZARRAT	1994.06.20	5.9	310.5	20
ZANJIRAN	ZANJIRAN	1994.06.20	5.9	886.8	14.4
ZANJIRAN	SERVESTAN	1994.06.20	5.9	12.6	20
	HOSSEINEH OLYA	1994.07.31	5.3	163.8	17.8
SAREIN	NIR (KARSHENASI)	1997.02.28	6.1	38.7	15.6
SAREIN	KARIQ	1997.02.28	6.1	494.3	15.4
	NAMIN	1997.03.02	5	24.1	19.8
	HASHTPAR	1998.07.09	5.5	14	17.9
	DAM (SATARKHAN)	1998.07.11	5.5	15.1	17.3

	MALAKSHAHI	1998.08.05	4.9	12.1	19
	KOHNUSH	1998.08.28	4.5	18	19.4
	MARUN DAM	1999.01.29	4.5	24.3	19.4
	BABAKALAN	1999.01.29	4.5	14.1	18.8
	BEHBAHAN	1999.01.29	4.5	12.1	18.1
	ABAD	1999.09.25	4.6	19.6	18.9
	DELVAR	1999.09.25	4.6	9.7	18.4
POL-E-ABGINEH	KAZEROON	1999.10.31	4.9	70.7	18.8
POL-E-ABGINEH	ROMGHAN	1999.10.31	4.9	13.8	18.1
POL-E-ABGINEH	BALADEH	1999.10.31	4.9	59.9	18.1
	GORGAN	1999.11.26	4.6	11	19.6
	BARDESKAN	2000.03.28	4.8	21.9	20
	SEPIDAN	2000.06.23	4.5	15.2	18.6

Table 4: List of training earthquake records, 30 sec duration, Site geology: Rock [31]

Earthquake	Station	Date	Magnitude M_S	Modified PGA (cm/sec^2)	Duration (sec)
	MAKU	1976.11.24	7.3	91.5	28
	SEDEH	1979.01.16	6.8	41.2	28
	TABAS	1980.01.12	5.8	160.8	28.6
	FIRUZABAD	1994.06.20	5.9	239	22
ZANJIRAN	MOHARLO	1994.06.20	5.9	22.3	25
SAREIN	NIARAQ	1997.02.28	6.1	23	25.4
SAREIN	NAMIN	1997.02.28	6.1	71.1	29.8
SAREIN	KHK (FARMD)	1997.02.28	6.1	18.9	21.8
SAREIN	KJH(BAHK.)	1997.02.28	6.1	8.3	23
	NIR	1998.07.09	5.5	18.6	23.2
	AHAR	1998.07.09	5.5	19.1	25.6
	NIARAGH	1998.07.09	5.5	32.8	20.5
	DAMIRCH	1998.07.13	5.5	41	24
	BAHAR	1998.08.22	4.5	9.8	21.7
	BORUJARD	1998.08.23	4.5	13	22.2
	SFANDAN	1998.08.28	4.5	15.4	23
	SFANDAN	1998.08.29	4.5	15.4	22.6
	PATAVEH	1998.09.21	4.6	56.3	25.6
	FEDAGH	1998.11.13	5.1	18.7	24
KAREBAS	SHABANKAREH	1999.05.06	6.3	10.7	23
KAREBAS	ABAD	1999.05.06	6.3	8.1	26.9
KAREBAS	DELVAR	1999.05.06	6.3	10.2	23
KAREBAS	KAVAR	1999.05.06	6.3	10.8	24.3
KAREBAS	MAHARLO	1999.05.06	6.3	13.1	24.3
KAREBAS	ZARRAT	1999.05.06	6.3	10.6	26.9
	ABAD	1999.09.24	4.7	47.9	26.2
	DELVAR	1999.09.24	4.7	100.3	24.3
POL-E-ABGINEH	GHAEMIYEH	1999.10.31	4.9	50.9	23.1
	MARAVEHTAPEH	1999.11.26	4.6	9.9	23
	RAZ	2000.08.22	5.8	62.5	24.8

Table 5: List of training earthquake records, 40 sec duration, Site geology: Rock [31]

Earthquake	Station	Date	Magnitude M_S	Modified PGA (cm/sec^2)	Duration† (sec)
TABAS	DEYHUK	1978.09.16	7.3	296.8	40
TABAS	TABAS	1978.09.16	7.3	817.8	38
	TORBATHYDARIYEH	1979.11.27	7.3	45.7	39.8
	BAJESTAN	1979.11.27	7.3	110.9	32.6
	SEDEH	1979.11.27	7.3	82.2	38
	KHAF	1979.11.27	7.3	129.2	40
Manjil-Rudbar	AB-BAR	1990.06.20	7.4	557.7	35
	Shabankareh	1996.01.24	4.5	53.4	32.3
SAREIN	RAZI	1997.02.28	6.1	34.4	32.8
SAREIN	HUR(BAKH.)	1997.02.28	6.1	58.7	37.4
	PSA	1998.07.09	5.5	41.2	36.7
KAREBAS	KAZEROON	1999.05.06	6.3	28.2	36.8
KAREBAS	CHENARSHAHIJAN	1999.05.06	6.3	36.1	40
Changureh-Avaj	BAHAR	2002.06.22	6.4	32.8	34.5
Changureh-Avaj	NAHAVAND	2002.06.22	6.4	25.8	36.4
BAM	Sirch	2003.12.26	6.7	30	40
BAM	Andoohjerd	2003.12.26	6.7	30.7	32
	AB-BAR	2004.05.28	6.3	34.8	40
SILAKHOR	Nahavand	2006.03.31	6.4	18	32.8
SILAKHOR	Hamedan5	2006.03.31	6.4	23.8	37.8

Table 6: List of training earthquake records, 20 sec duration, Site geology: Soil [31]

Earthquake	Station	Date	Magnitude M_S	Modified PGA (cm/sec^2)	Duration (sec)
	RUDSAR	1980.12.03	4.7	105.4	18.3
	RAVAR	1981.07.28	7	65.7	14.4
	GOLBAF	1989.11.20	5.7	293.73	12.1
Manjil-Rudbar	ROUDSHOR	1990.06.20	7.7	41.2	18
	MEIMAND	1994.06.18	5.7	401.7	16.6
SAREIN	MIYANEH	1997.02.28	6.1	12	20
	KHOMARLU	1998.07.09	5.5	16.2	19.42
	KALEYBAR	1998.07.09	5.5	12	20
	ASL	1998.07.09	5.5	12.5	17.9
	EKBATAN DAM	1998.08.21	4.5	10.1	16.66
	GIUAN	1998.08.21	4.5	24.6	19.34
SALEHABAD	GONBADLI	1998.11.08	5.2	17.2	18.94
	JOSHAN	1998.11.18	4.9	20	19.72
	KERMAN	1998.11.18	4.9	24.8	19.42
	GUYOM	1999.05.06	5.7	11.3	18.86
	BABAMONIR	1999.05.06	6.3	38.6	20
POL-E-ABGINEH	NURABADMAMASANI	1999.10.31	4.9	14.9	19.86
	KALALEH	1999.11.19	5.1	11.2	20
	ALIABAD	1999.11.26	4.6	303.3	13.62
	KASHMAR	2000.02.02	5.3	17.5	20
	KASHMAR	2000.03.28	4.9	12.4	19.76
	BEHSHAHR	2000.08.16	4.5	8.7	20
	B-TORKAMAN	2000.08.16	4.5	23.03	18.98
	RAZ	2000.09.19	4.7	23	19.76
Changureh-Avaj	AVAJ	2002.06.22	6.4	495.9	13
KAHAK	Gazoran	2007.06.18	5.4	77.2	19.7
KAHAK	Hassan Abad	2007.06.18	5.4	38.6	19.94

KAHAK	Shahriyar	2007.06.18	5.4	9.8	19.86
KAHAK	TEHRAN 11	2007.06.18	5.4	11.5	19.72
KAHAK	Qani Abad	2007.06.18	5.4	14.7	18.2

Table 7: List of training earthquake records, 30 sec duration, Site geology: Soil [31]

Earthquake	Station	Date	Magnitude M_S	Modified PGA (cm/sec^2)	Duration (sec)
	GHAEN	1979.11.27	7.3	195.4	29.28
ZANJIRAN	BABANAR	1994.06.20	5.9	28.2	24.24
SAREIN	MESHKINSHAHR	1997.02.28	6.1	25.2	28.1
SAREIN	GERMY (KARSHENASI)	1997.02.28	6.1	43.5	25.7
	HERIS	1998.07.09	5.5	15.4	29.54
	BOJNORD	1998.08.04	5.1	29.3	24.26
	SALEHABAD	1998.08.05	4.9	27.9	22.96
	BEYRAM	1998.11.13	5.1	10.2	22.9
	EVAZ	1998.11.13	5.1	27.5	27.1
	KERMAN	1998.11.18	4.9	19.7	24.18
	DEHDASHAT	1999.01.29	4.5	45.7	29.32
	BANDARABAS	1999.03.04	6.4	15.3	26.8
KAREBAS	KAPHTARAK	1999.05.06	6.3	14.6	26.14
KAREBAS	ZARGHAN	1999.05.06	6.3	11.2	21.74
KAREBAS	SHIRAZ 3	1999.05.06	6.3	14.1	26.9
KAREBAS	SHIRAZ 2	1999.05.06	6.3	28.96	29.6
KAREBAS	SHIRAZ (GEO)	1999.05.06	6.3	14.1	27
SALEHABAD	NASRABAD	1999.11.08	5.2	15.7	26.86
	RAMIYAN	1999.11.19	5.1	24.4	30
	VOSHMGIR	1999.11.19	5.1	39.6	29.32
	MOHAMADABAD	1999.11.19	5.1	10.2	23.02
	AGHGHALA	1999.11.19	5.1	31.7	29.76
	AGHBAND	1999.11.19	5.1	13.5	27.88
	OROMIYEH	2000.06.26	5.2	16.9	21.54
Changureh-Avaj	GILVAN	2002.06.22	6.4	17.4	26.82
Changureh-Avaj	GHAHAVAND	2002.06.22	6.4	24.4	30
Bam	Shahdad	2003.12.26	6.7	19.9	30
Bam	Bam	2003.12.26	6.7	759.6	26.96
KAHAK	Panzdahe khordad	2007.06.18	5.4	41.6	28.38
KAHAK	Naragh	2007.06.18	5.4	20.6	29.9

In the previous work, some researchers use pseudo-velocity response spectrum (PSV) as inputs [2,6] and others use pseudo-velocity response acceleration (PSA) [7]. In this research, both PSV & PSA used for training ANNs separately, to compare the results and recognizing that which of them is more suitable for our purpose. The values of the response spectrums of accelerograms calculated at 1000 discrete frequencies according to the following formula [23]:

$$\ddot{x}(t) + 2\zeta\omega_l \dot{x}(t) + \omega_l^2 x(t) = -a_g(t), \tag{15}$$

$$PSV(\omega_l, \zeta) = \omega_l \max_t |x(t)|, l = 1, 2, 3, ..., 1000, \quad \zeta = 5\%, \tag{16}$$

$$PSA(\omega_l, \zeta) = \omega_l PSV(\omega_l, \zeta) = \omega_l^2 \max_t |x(t)|, l = 1, 2, 3, ..., 1000, \quad \zeta = 5\%, \tag{17}$$

where ω_1 , ζ and $a_g(t)$ are the fundamental frequency and the damping coefficient of the single degree of freedom system and the earthquake ground acceleration, respectively.

Table 8: List of training earthquake records, 40 sec duration, Site geology: Soil [31]

Earthquake	Station	Date	Magnitude M_S	Modified PGA (cm/sec^2)	Duration (sec)
	KHAF	1979.11.14	6.7	80.95	38.9
	GONABAD	1979.11.27	7.3	73	39.94
	KHEZRI	1979.11.27	7.3	95.1	35.02
	KERMAN	1981.07.28	7	98.2	37.92
Manjil-Rudbar	ESHTEHARD	1990.06.20	7.4	76.5	40
GARMKHAN	BAREZO DAM	1997.02.04	6.8	41.6	35.76
SAREIN	ARDEBIL 1	1997.02.28	6.1	109.1	40
SAREIN	ASTARA	1997.02.28	6.1	42.8	40
SAREIN	ARDEBIL(MASKAN)	1997.02.28	6.1	160.2	39.3
GOLBAF	KERMAN 2	1998.03.14	6.9	40.1	39.5
GOLBAF	KERMAN 1	1998.03.14	6.9	35.5	37
	BIRJAND	1998.04.10	5.7	16.6	34.26
	MESHKINSHAHR	1998.07.09	5.5	22.7	31.98
	LALEHZAR	1999.03.04	6.4	15.3	33.26
KAREBAS	GUYOM	1999.05.06	6.3	37.2	36.52
KAREBAS	BABAMONIR	1999.05.06	6.3	13.4	39.66
Changureh-Avaj	BOOEIN ZAHRA	2002.06.22	6.4	18.7	40
Changureh-Avaj	ABHAR	2002.06.22	6.4	38.7	40
Changureh-Avaj	ESHTEHARD	2002.06.22	6.4	18.3	31.94
Bam	Joshan	2003.12.26	6.7	24.4	39.66
Bam	Kerman1	2003.12.26	6.7	18.3	38.86
Bam	Mohamad Abad	2003.12.26	6.7	117.9	38.44
Bam	Ravar	2003.12.26	6.7	12	38.38
Bam	Lale Zar	2003.12.26	6.7	12.8	35.36
Kojur Firoozabad	Tonekabon	2004.05.28	6.3	45.9	39.88
Silakhor	Khoram Abad	2006.03.31	6.4	35.3	39.89
Silakhor	Khondab	2006.03.31	6.4	50.9	36.48
KAHAK	Mamooniyeh	2007.06.18	5.4	34.6	40
KAHAK	Veshnaveh	2007.06.18	5.4	38.9	39.94
KAHAK	Raveh	2007.06.18	5.4	21.7	33.94

According to the above calculations, input layers of ANNs will have 1,000 neurons that it would make impossible to training and converging ANNs. Therefore, with the usage of PCA these values will reduce to a reasonable number by a high precision.

Wavelet packet coefficients of accelerogram ($a_g(t)$) are embedded in the inner product of the signal with every wavelet packet function, denoted by $c_j^i(k)$ and calculated as follow:

$$c_j^i(k) = \sum_l a_g(t)\,\omega_{j,n}^k(t), \tag{18}$$

where $c_j^i(k)$ denotes the ith set of wavelet packet decomposition coefficients at the jth scale parameter and k is the translation parameter.

The wavelet packet components of accelerogram $a_j^i(t)$ represented by a linear combination of wavelet packet functions $\omega_{j,n}^k(t)$ as follows:

$$a_j^i(t) = \sum_l c_j^i(k)\,\omega_{j,n}^k(t). \tag{19}$$

After *j* level of decomposition, the original signal $a_g(t)$ can be reconstructed as [6]:

$$a_g(t) = \sum_{i=1}^{2^j} a_j^i(t). \tag{20}$$

WPCs of accelerograms computed with Shannon-Entropy at appropriate WPT decomposition level, j, with db-10 wavelet, although other wavelets would not make any significant change in the results. PCA is not reliably reversible. Therefore, we apply it only on inputs (PSA or PSV) and outputs (WPCs) will apply to ANNs without any modifications.

6.2. ANN Training and Testing phase

As mentioned before the main subject of this paper is the using ANNs to mapping a relation between response spectrum of training accelerograms that compact with PCA and WPCs of them. The training procedure of a neural network has two separate stage: first specifying the network's architecture that includes the number of hidden layers, the number of nodes in each layer and the activation functions of hidden and output layers; second modifying the weights and biases of ANNs so the difference between outputs of ANN and targets being less than a specified amount.

In this study, all ANNs have only one hidden layer, also the number of neurons at hidden layer determined according to the number of nodes at input and output layers and experience. For enabling ANNs to make a nonlinear relation between inputs and outputs the activation functions of hidden layers are 'tansig' and because outputs (WPCs) have a wide range values, the activation functions of outputs layers are 'purelin'.

BP algorithms, that are gradient descent in essence, are the most widely used search technique for evolving weights and biases of MLFF. One of characteristics of the gradient descent algorithms is rapid convergence on the local optima. Another problem that encountered when using BP is that, when the number of neurons of various layers increased, the time of evolving ANN increase rapidly. For overcoming these drawbacks, first ACO algorithm is used to locating the parameters of ANNs in the near of their optimum value so ANNs escape from overfitting and then BP algorithm is used to find the accurate parameters.

6.2.1. ACO for neural network optimization

Many researchers use ACO for optimizing ANNs in many science aspects [24-26]. Figure 2 gives the flow chart of the algorithm.

The detail of ACO for ANN optimization is as follows:

1) Initialization. Create a pheromone table for each parameter (biases and weights) and

all values have the same amount of pheromone τ_0.

2) Release ants. Each ant selects a value for each parameter according to their pheromone value and probability such as:

$$P(i) = \frac{\tau(i)}{\sum_{1 \le j \le m} \tau(j)}. \tag{21}$$

For the first iteration all values selected randomly.

3) Compute each ant's solution cost. When all ants select a matrix for biases and weights of ANN, cost for kth ant is compute as follow:

$$L(k) = \frac{1}{2} \sum_{s=1}^{P} \sum_{i=1}^{N_M} (d_{s,i} - y_{s,i}^{M})^2, \tag{22}$$

where $d_{s,i}$ and $y_{s,i}^{M}$ are the ith target and actual outputs corresponding to the sth training pattern respectively, N_M is the number of output units and P is the number of training samples.

4) Check termination criterion. If algorithm reaches to its maximum iteration or the best ant's solution reach to precision or all the ants converge on one path, set NN parameters to the bests that find in algorithm and evolving the network using BP algorithm. Else, start next iteration.

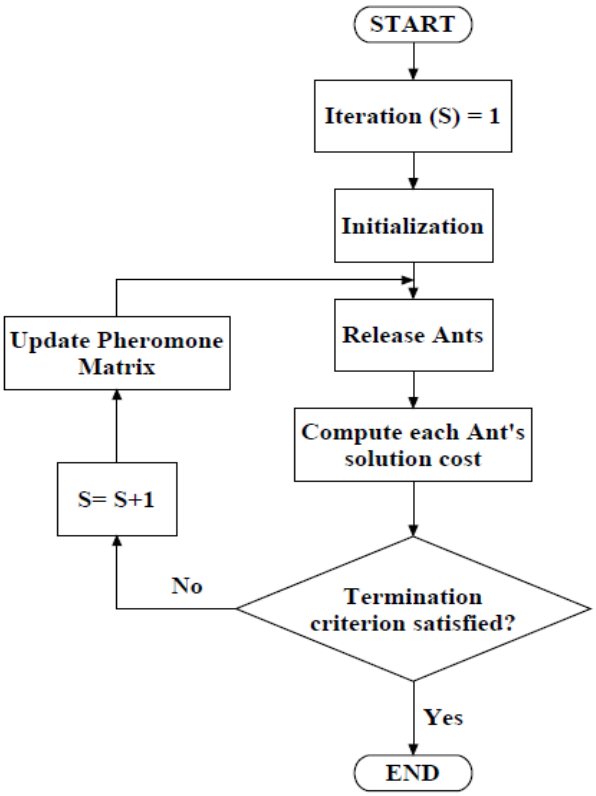

Figure 2. Basic flowchart of ACO for ANN optimizing

5) Update pheromone matrix. After computing all ants' cost update pheromone matrix according to the following formula:

$$\begin{cases} \tau(t+1) = \rho \times \tau(t) + \dfrac{Q}{L(k)}, \text{if value is selected by } k_{th} \text{ ant for } m_{th} \text{ parameters} \\ \tau(t+1) = \rho \times \tau(t), \text{if value is not selected by } k_{th} \text{ ant for } m_{th} \text{ parameters} \end{cases} \quad (23)$$

6.2.2. Evolving the network using BP algorithm

Set the best parameters that founded by ACO algorithm as the initial weighs and biases of ANNs, and using BP algorithm to finding the exact values. 'tansig' that used as the transfer function of hidden layers is a sigmoid function. These types of functions are called "squashing" functions, because they compress an infinite input range into a finite output range. Sigmoid functions are characterized by the fact that their slopes should approach zero, as the input gets large. This causes a problem when the steepest descent is used to train a multilayer network with sigmoid functions, because the gradient can have a very small magnitude and, therefore, it may cause small changes in the weights and biases, even when the weights and biases are far from their optimal values [27].

Therefore, for better and faster training of ANN, we use resilient backpropagation (Rprop) algorithm for evolving the ANNs parameters. Rprop performs a direct adaptation of the weight step based on local gradient information. This algorithm, apply an individual update-value for each weight (Δ_{ij}), which solely determines the size of the weight-update. This adaptive update-value evolves during the learning process based on its local sight on the error function (E), according to the following learning rule:

$$\Delta_{ij}^{(t)} = \begin{cases} \eta^{+} \times \Delta_{ij}^{(t-1)}, \; if \; \dfrac{\partial E^{(t-1)}}{\partial w_{ij}} \times \dfrac{\partial E^{(t)}}{\partial w_{ij}} > 0 \\ \eta^{-} \times \Delta_{ij}^{(t-1)}, \; if \; \dfrac{\partial E^{(t-1)}}{\partial w_{ij}} \times \dfrac{\partial E^{(t)}}{\partial w_{ij}} < 0 \\ \Delta_{ij}^{(t-1)}, else, \end{cases} \quad (24)$$

where $0 < \eta^{-} < 1 < \eta^{+}$ that increase or decrease the update value.

Once the updated value for each parameter is adapted, the parameter updates itself according to a very simple rule: if the derivative is positive (increasing error), the parameter is decreased by its updated value, if the derivative is negative, the updated value is added, and if the partial derivative changes sign, the previous updating weight is reverted [28]:

$$\Delta w_{ij}^{(t)} = \begin{cases} -\Delta_{ij}^{(t)} \ , \ if \ \ \dfrac{\partial E^{(t)}}{\partial w_{ij}} > 0 \\ +\Delta_{ij}^{(t)} \ , \ if \ \ \dfrac{\partial E^{(t)}}{\partial w_{ij}} > 0 \\ -2 \times \Delta w_{ij}^{(t-1)} \ , \ if \ \dfrac{\partial E^{(t-1)}}{\partial w_{ij}} \times \dfrac{\partial E^{(t)}}{\partial w_{ij}} < 0 \\ 0, else, \end{cases} \tag{25}$$

$$w_{ij}^{(t+1)} = w_{ij}^{(t)} + \Delta w_{ij}^{(t)} \tag{26}$$

6.2.3. Testing the ANN

After completing the training phase and all ANNs reached to desire performance, the trained ANNs were tested by presenting the response of accelerograms as input and comparing them with the ANNs accelerograms that derived by applying Inverse Wavelet Packet Transform (IWPT) to the outputs of networks. These comparisons first performed for the accelerograms in the training set, and if ANNs produced the same accelerograms, next a novel accelerograms which were not included in the training set is apply to the networks. With these actions we can certain that ANNs learned their learning patterns, could generate reasonable response to new inputs, and are not overfitting.

If ANNs do not pass the testing phase, training phase start again with new conditions for ACO algorithm.

6.3. Artificial Earthquake Records Generation stage

If ANNs passed the training phase, they used for generating an artificial earthquake record that its response spectrum is closely matched the input spectrum. This is a useful property of the neural network based method, which it will enable to generate of accelerograms compatible with any defined design spectra. The generated accelerograms can then used in time history analysis of linear and nonlinear structures.

For applying a desire response spectrum to ANNs, first real values of it transform to virtual relevant ones by using PCA and then these compact values applied to the ANNs to get their response. For generating multiple artificial earthquake records, a Gaussian noise applies to the outputs of the hidden and output layers. This method used by the other researchers, and allows the ANNs to generate accelerograms with same nature but different time history and response spectrum. So the output of neurons at hidden and output layers calculated as follow:

$$Out_i = f\left(\sum_j W_{ji}.X_i + b_i\right) + \varepsilon, \tag{27}$$

where Out_i, f, $W_{ji}.X_i$ and b_i are the output, transfer function, input and bias of ith neuron,

respectively and $\varepsilon \sim N(0,\sigma^2)$ (the activation randomness parameter) is a Gaussian distributed random noise having zero mean and σ^2 variance [2].

After generating artificial earthquake records by using IWPT to the outputs of ANNs, for more spectrum matching, detailed coefficients of artificial accelerograms that obtained by using discrete wavelet transform are modified by the Eq. 28 or 29:

$$cD_j^{Mod} = cD_j \times \frac{\int_{T_{1j}}^{T_{2j}} PSA(T)_{Tar}\, dT}{\int_{T_{1j}}^{T_{2j}} PSA(T)_{Calc}\, dT}, \tag{28}$$

$$cD_j^{Mod} = cD_j \times \frac{\int_{T_{1j}}^{T_{2j}} PSV(T)_{Tar}\, dT}{\int_{T_{1j}}^{T_{2j}} PSV(T)_{Calc}\, dT}, \tag{29}$$

$$T_{1j} = 2^j \Delta t \qquad T_{2j} = 2^{j+1} \Delta t, \tag{30}$$

where T_{1j} and T_{2j} are boundary values of period range for level j in DWT and Δt is the time step of artificial accelerograms. Moreover, $PSA(T)_{Calc}$ ($PSV(T)_{Calc}$) is artificial PSA (PSV) at period T that is computed from nonaligned artificial accelerogram and $PSA(T)_{Tar}$ ($PSV(T)_{Tar}$) is artificial PSA (PSV) at period T [29,30].

The complete flowchart of proposed method illustrated in Figure 3.

7. INTERPRETIVE EXAMPLES

187 earthquake accelerograms that recorded in Iran are used for training the ANNs, that all of these records were discretized at 0.02 sec. [31]. Therefore, all accelerograms with durations of 10, 20, 30, and 40 sec. have 501, 1001, 1501, and 2001 discrete points, respectively. Tables 2 to 8 show the list of training records in each soil condition and duration group.

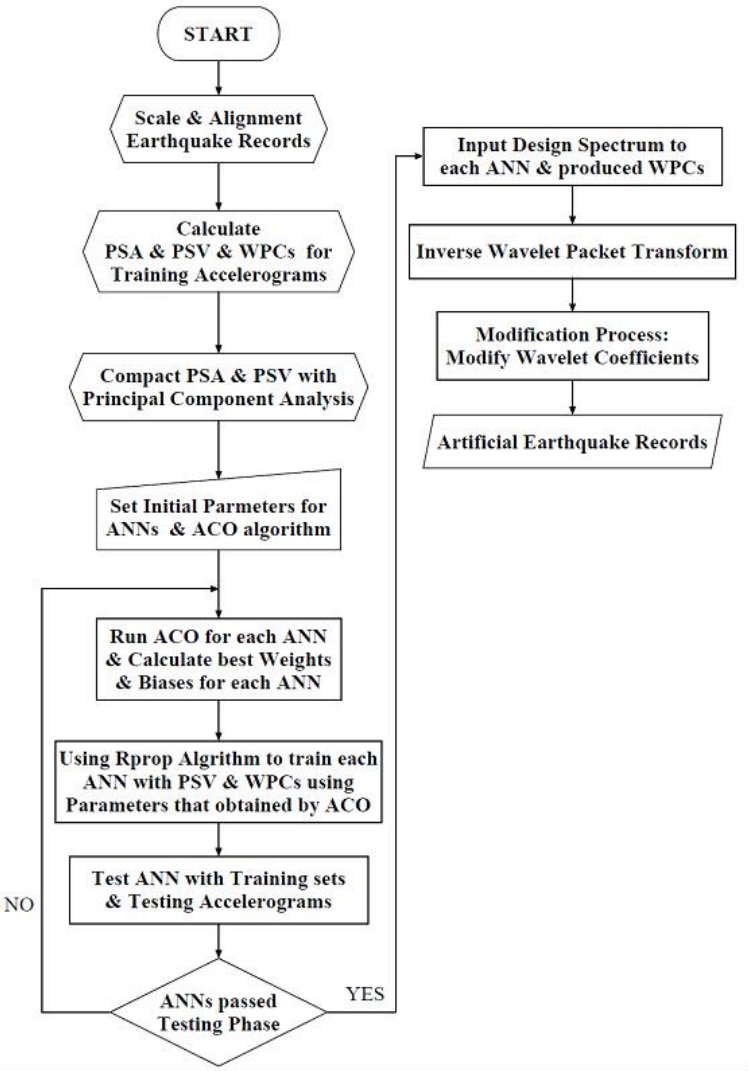

Figure 3. Complete flowchart of proposed method

PSA or PSV spectra of all accelerograms are calculated numerically, according to Equations 15 to 17 at 1000 equally spaced discrete period in the range of 0.01-10s, with 5% damping ratio (ζ=5%). For reducing the dimension size of PSA (PSV), different effective variance ratios is selected as $R_{eff}^{\text{var}} = 0.999\%$, so the number of neurons in input layers of ANNs are according to Table 9.

As mentioned before, the output layer of neural networks has the wavelet packet coefficients at level *j* of the wavelet packet transform of the earthquake accelerograms.

Appropriate decomposition levels selected according to different parameters such as the accelerogram's duration, total WP packs coefficient numbers, desired precision in spectrum compatibility and the reasonable computational time in training ANNs. Therefore, the number of nodes at output layers of the ANNs, and the number ANNs that should trained, are determined after decomposition of accelerogram, and are according to Table 10.

Table 9: Number of Neurons in ANNs' input layers

Duration Group	No. of Input Neurons
Soil Condition: **Rock**	
10	27
20	31
30	34
40	25
Soil Condition: Soil	
20	35
30	35
40	35

Table 10: Number of packs and WP coefficients in each duration group

Duration Groups	Selected Levels of Decomposition in WPT	Number of Packs (No. of ANNs)	Number of Coefficients in each Pack (No. nodes in Output layer)
10 sec.	5	32	34
20 sec.	6	64	34
30 sec.	7	128	30
40 sec.	7	128	34

Other parameters of neural networks architecture are transfer functions of layers and the number of neurons in hidden layers. Criterion of the selection of transfer functions discussed at section 6.2. The number of neurons at hidden layer varied from 35 to 43 according to the number of neurons at input and output layer and experience.

ACO as a metaheuristic algorithm has the advantage of global optimization and easy realization. Optimum state of using ACO derived only by selecting appropriate value for algorithm parameters. The important parameters that should define for algorithm are evaporation rate, number of explorer ants and initial pheromone value. The evaporation rate (ρ) enables the ants to forget the old solution and explore the new path. Usually ρ sets as to 0.8-0.95, so we choose 0.9 in all algorithms.

A large number of ants (N) can endow algorithm with powerful ability of exploring more candidate solutions in an iteration, but it is at the expense of more CPU time in the case of nonparallel realization. A small N is not good for exploring new paths, especially in the later phase of ACO algorithm [32]. In this study, we use 40-60 ants according to our desire precision.

If initial pheromone value (τ_0) is selected too low, then the search is quickly biased by the first solutions generated by the ants, on the other side, if τ_0 is too high, then many iterations are lost waiting until pheromone evaporation reduces enough pheromone values, so that pheromone added by ants can start to bias the search. For our purpose, we find the best value for τ_0 according

to trial and error procedures and TSP references.

By completion the training phase of ANNs, the trained neural networks tested with the records from the training group. Figures 4 and 5 show a test of the trained neural networks for 10 and 40 seconds duration in Rock training set and figure 6 shows another one for 30 seconds duration in Soil training set, respectively. The left side of each figure shows the result of ANNs that trained by PSV and the right shows the response of PSA's ANNs.

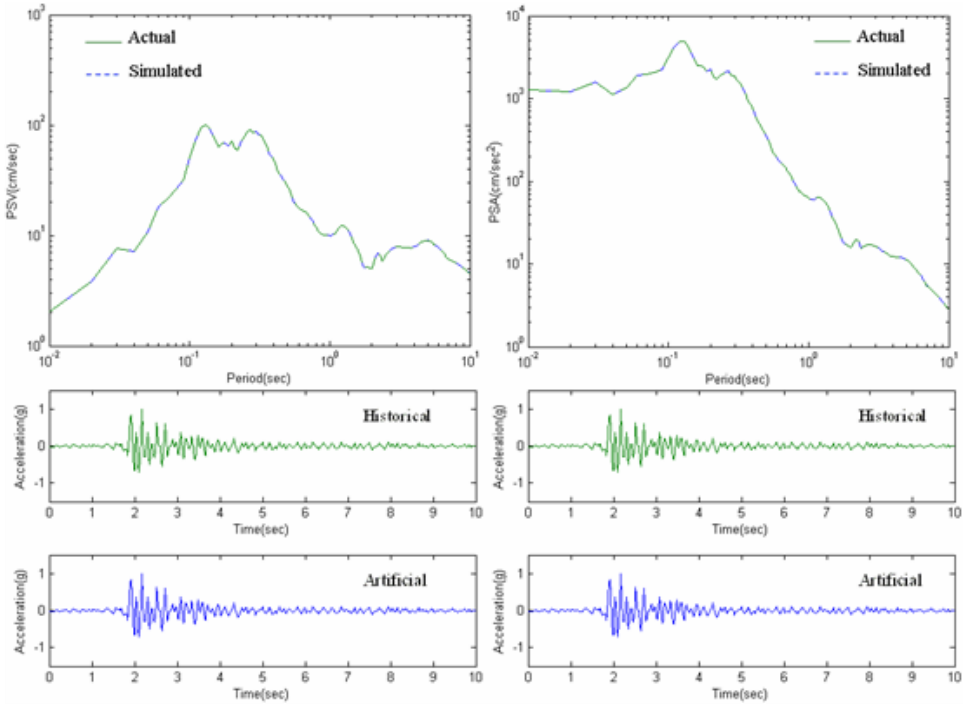

Figure 4. A test of ANNs from the Rock training group with 10 sec. duration (Shalamzar Sta., 1984)

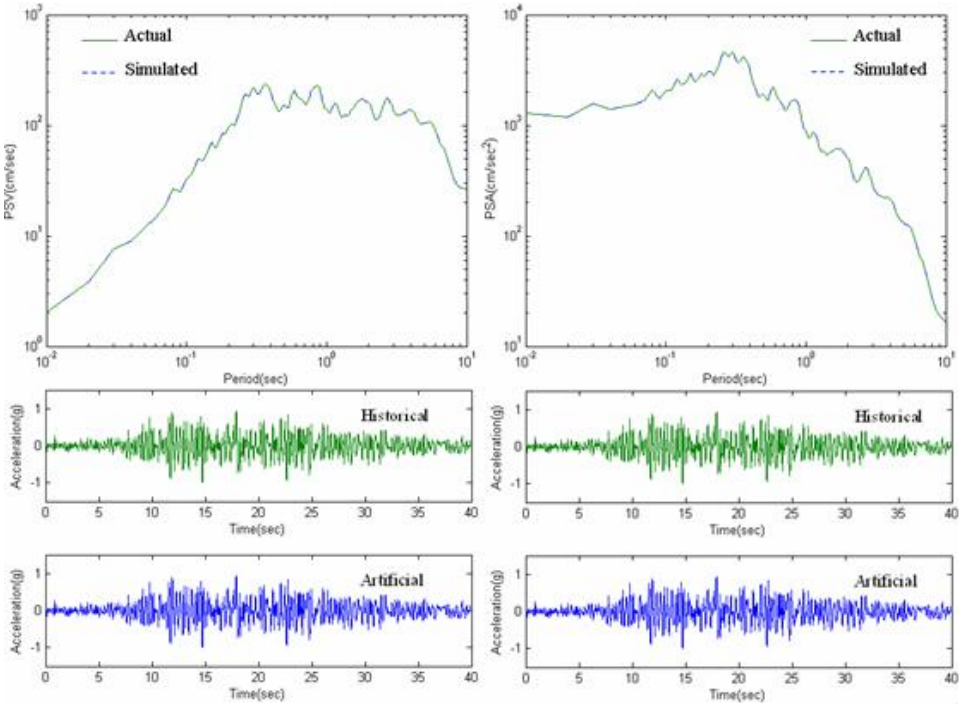

Figure 5. A test of ANNs from the Rock training group with 40 sec. duration (Torbat-hydariyeh Station, 1979)

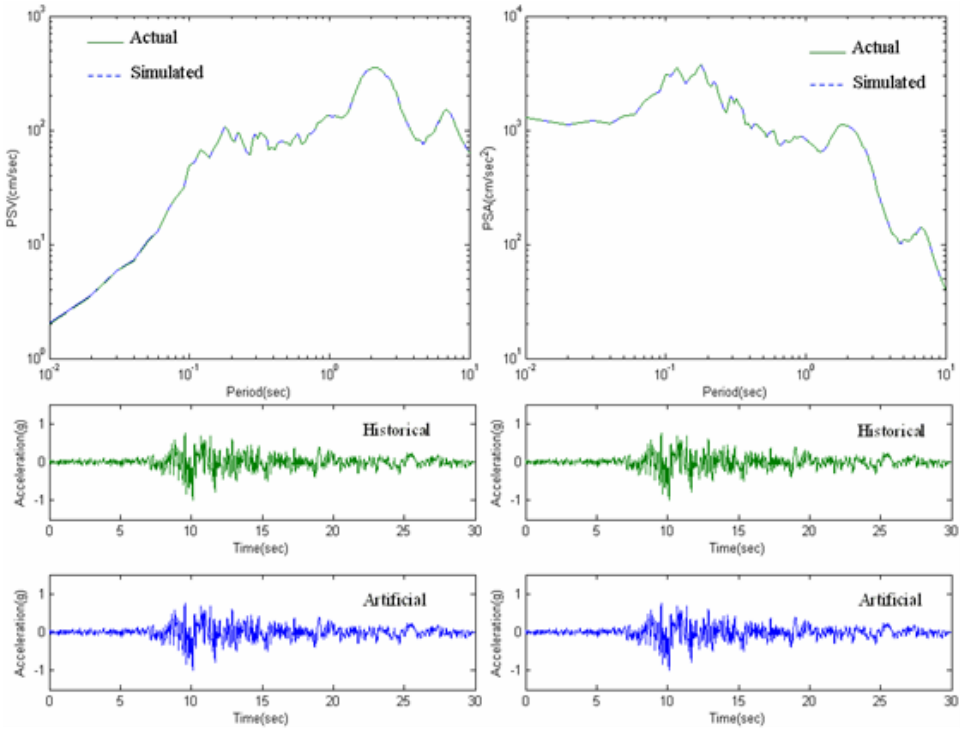

Figure 6. A test of ANNs from the Soil training group with 30 sec. duration (Shahdad Sta., 2003)

With comparison of the actual and generated accelerograms, and their response spectrums we can certain that the trained ANNs have learnt the training cases very well. Also the responses of ANNs that trained by PSA is completely alike that derived by PSV's ANNs.

After make sure that ANNs learnt their training path, they tested by accelerograms that are not participated in their training set. For having a numerical criterion for comparison the results of ANNs with truth and other work, we represent the difference between actual and simulated response spectra by use of root mean square error (RMSE). Figures 7 and 8 show a test of the trained neural networks for new records in Rock 20 and 30 seconds duration and figures 9 and 10 show the results of Soil 20 and 40 seconds, respectively. Note that, the RMSE that written below the each figure is the average of ANNs that trained by PSA or PSV. By comparing the response spectra of actual and simulated accelerograms, and the value of RMSE we could conclude that ANNs were able to generate appropriate outputs to the inputs that were not in their training sets.

After testing phase, the major purpose of this paper that is generation of multi artificial earthquake records that their spectrum matched a flat design spectrum can derive. The generated accelerograms are artificial accelerograms with similar characteristics as those in the training set and their response spectra are very close to the input design spectrum. A number of design spectra presented as novel cases to the trained ANNs. For example figures 11 and 12 show the generated varied duration accelerograms from Newmark and Hall [33] with PGA 1g and mean hazard level for *Rock* and *Soil* geology. As shown in training and testing figures the response of

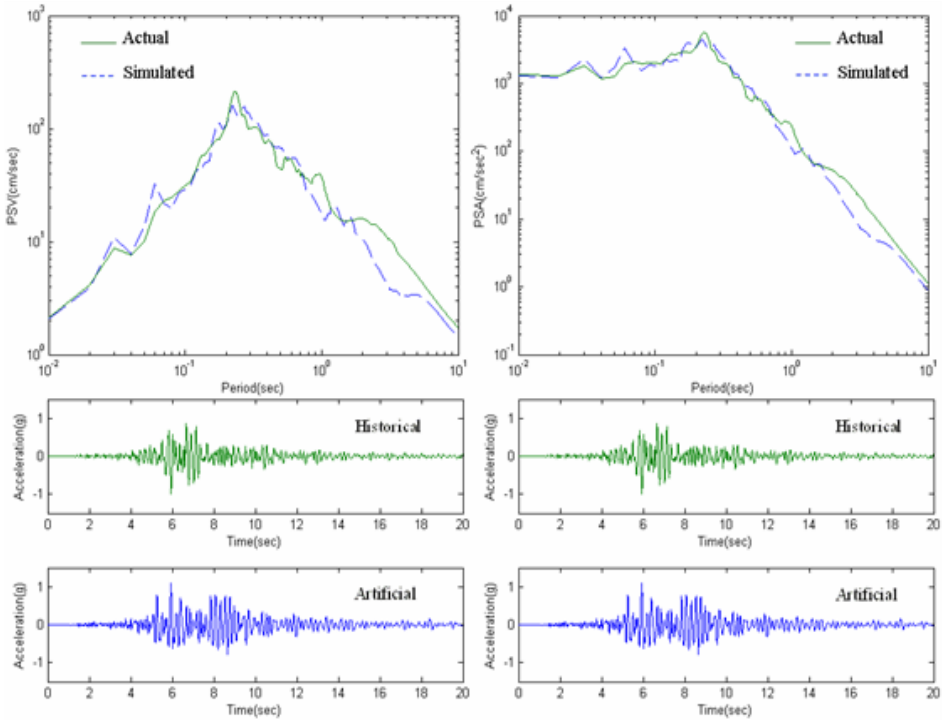

Figure 7. A test of ANNs by a new accelerogram in Rock group with 20 sec. duration (Zarrat Sta., 1994) (RMSE = 0.1732)

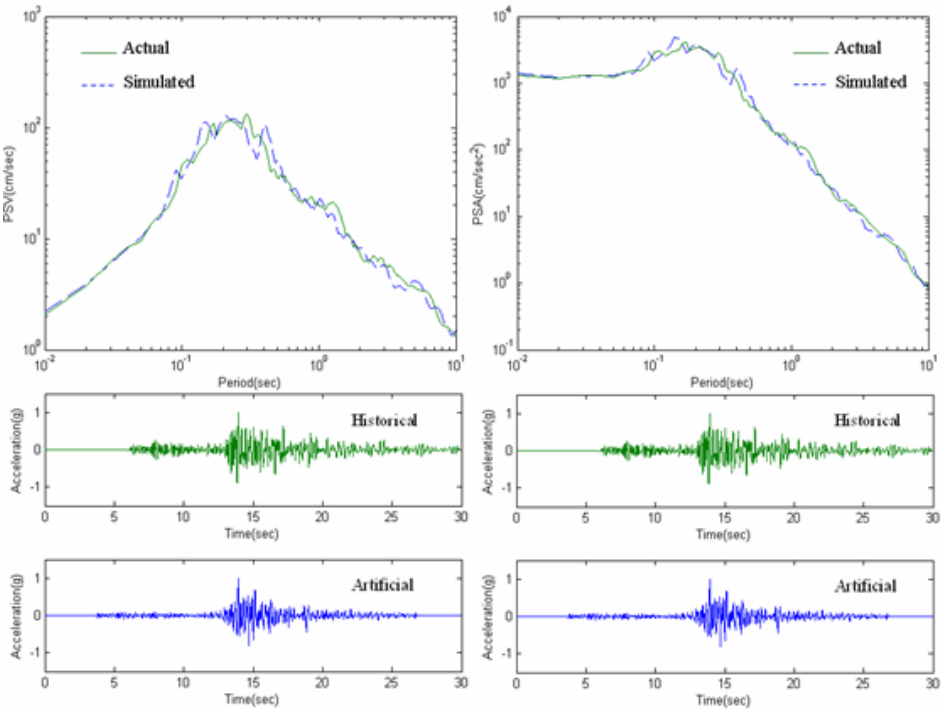

Figure 8. A test of ANNs by a new accelerogram in Rock group with 30 sec. duration (Selseleh Sta., 1998) (RMSE = 0.1016)

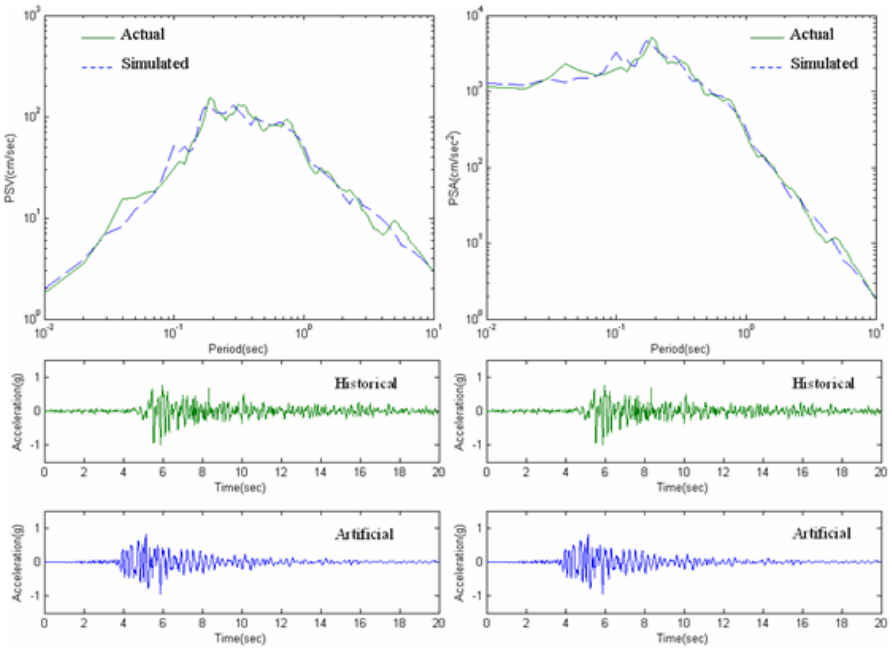

Figure 9. A test of ANNs by a new accelerogram in Soil group with 20 sec. duration (B-Torkaman Sta., 1999) (RMSE= 0.1269)

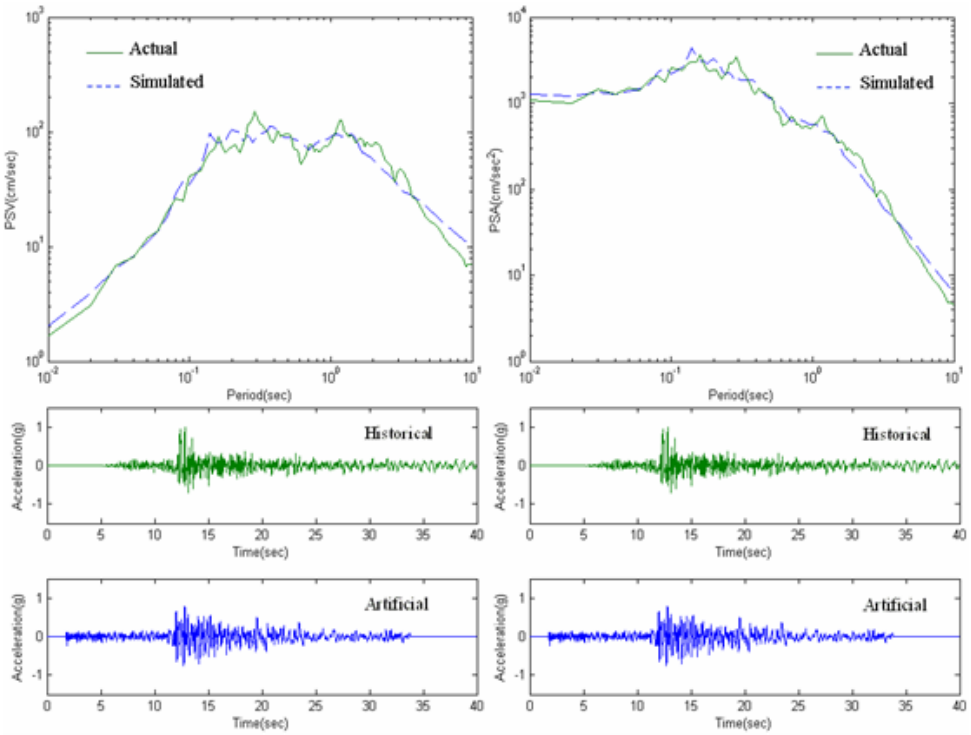

Figure 10. A test of ANNs by a new accelerogram in Soil group with 40 sec. duration (Gomeshan Sta., 1999) (RMSE= 0.1117**)**

ANNs that trained by PSA or PSV are completely similar, therefore the artificial time histories that derived from PSA's ANNs is just displayed.

Comparison between the target spectrum and the PSAs of artificial accelerograms shows that proposed method is capable of producing different but reasonable and realistic earthquake accelerograms from a desire design spectrum.

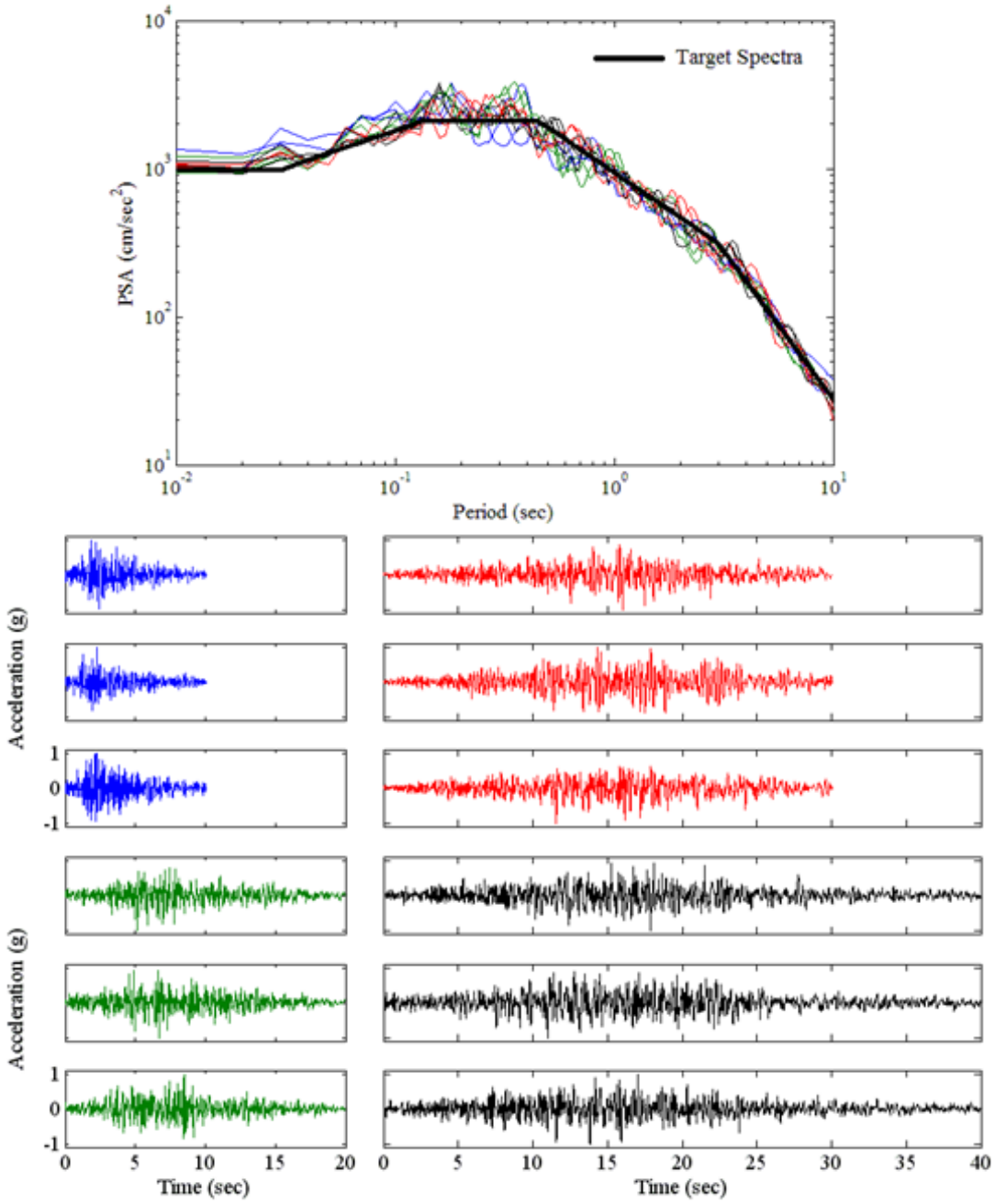

Figure 11. Generated earthquake accelerograms from the design response spectrum (mean-1.0g-Rock)

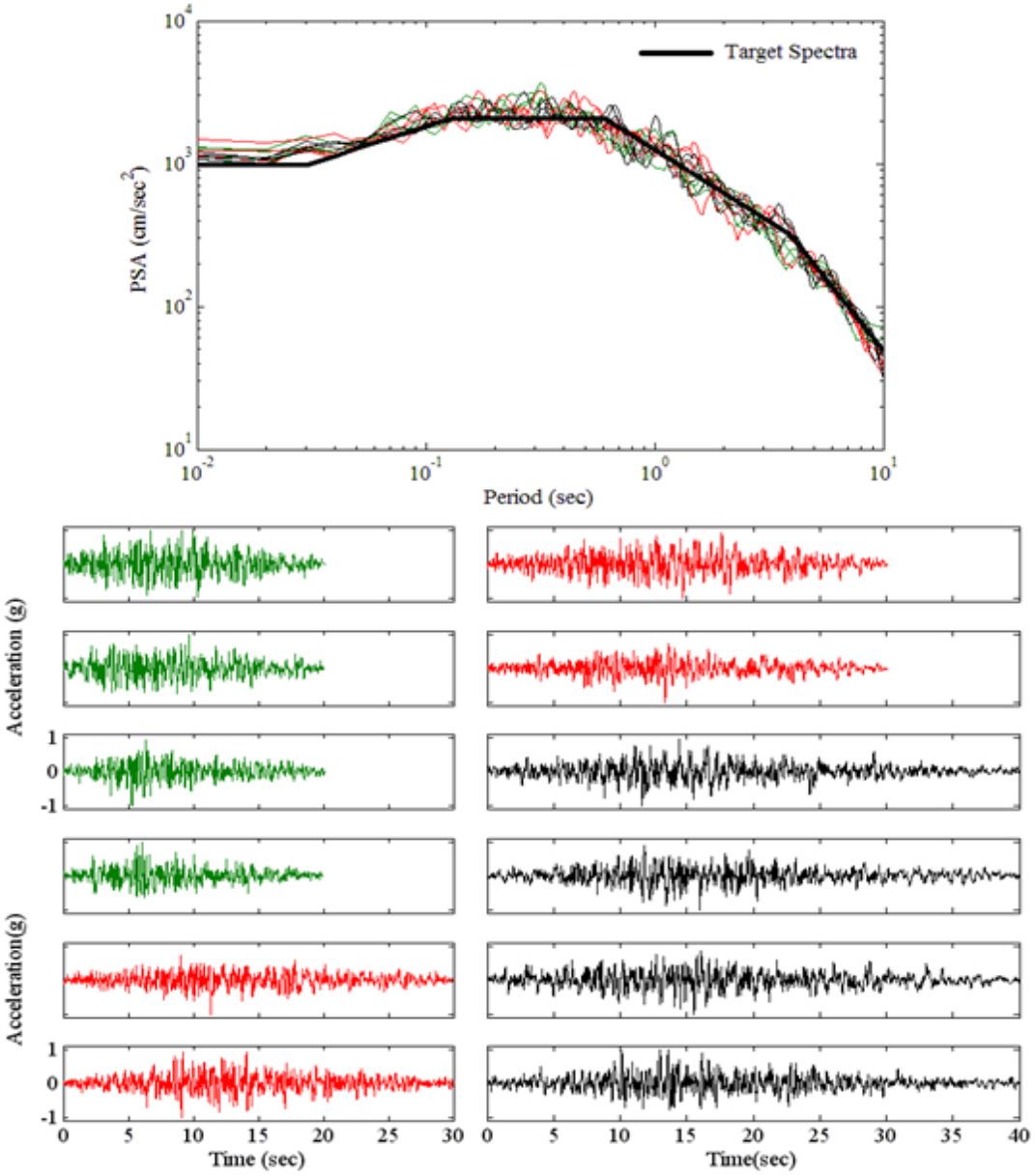

Figure 12. Generated earthquake accelerograms from the design response spectrum (mean-1.0g-Soil) (Average of RMSE= 0.1639)

8. CONCLUDING REMARKS

In this paper, hybrid artificial neural networks based on ACO-Rprop used for generating multiple spectrum-compatible artificial earthquake records for specified site geology. By using the learning capability of ANNs, an inverse mapping from response spectrum to wavelet packet coefficients at level j of the wavelet packet transform of the earthquake accelerograms is developed. Learning accelerograms categorized into Rock and Soil group

according to the shear velocity under their recorder stations. In addition, for having artificial records with varied durations and better resolution by using WPT, training sets categorized according to the bracket duration of accelerograms. So the proposed method is applied to a sample of 186 Iran recorded earthquakes categorized into two site geology and four duration groups 10, 20, 30, and 40 seconds. For overcoming the drawbacks of traditional ANN's learning algorithms and faster training, a hybrid algorithm base on ant colony optimization and Resilient backpropagation algorithm (Rprop) is presented, also by using the PCA for decreasing the number of nodes at input layers, maximum time that spends for training one ANN is eliminated to 150 seconds.

After completing the training phase of ANNs, they tested with accelerograms from the training sets and accelerograms that were not included in training set. If the inputs to ANNs are included in training sets, they should generate an accelerogram completely similar to input. However, when PSA or PSV of accelerogram, which were not included in the training set, used as Input, the neural networks may perform in two different ways. First, the neural network picks an accelerogram similar to one from its training set, if its response spectrum is close to the input response spectrum. Second, in case there are no earthquake records in the neural network's training set which have a response spectrum close to the input response spectrum, the trained neural network synthesizes a reasonable looking accelerogram from its training set.

After be certained that ANNs learned their learning path and could generate reasonable response to new inputs, artificial earthquake records derived by applying a desire design spectrum to ANNs' input layers and a Gaussian noise to hidden and output layers. As shown in the previous pictures, the response spectra of the generated accelerograms are closed to the design spectrum (average RMSE = 0.1594) and they have time domain characteristics as earthquake accelerograms.

REFERENCES

1. Ghaboussi J, Lin CC. New method of generating spectrum-compatible accelerograms using neural networks. *Earthquake Eng Struct Dynam*, 1998; **27**: 377-96.
2. Lin CC, Ghaboussi J. Generating multiple spectrum compatible accelerograms using stochastic Neural Networks. *Earthquake Eng Struct Dynam*, 2001; **30**: 1021-4.
3. Lee SC, Han SW. Neural-network-based models for generating artificial earthquakes and response spectra. *Comput Struct*, 2002; **80**: 1627-38.
4. Rajasekaran S, Latha V, Lee SC. Generation of artificial earthquake motion records using wavelets and principal component analysis. *J Earthquake Eng*, 2006; **10**(5): 665-91.
5. Ghodrati Amiri G, Bagheri A, Fadavi M. New method for generation of artificial ground motion by a nonstationary Kanai-Tajimi model and wavelet transform. *Struct Eng Mech*, 2007; **26**(6): 709-23.
6. Ghodrati Amiri G, Bagheri A, Razaghi SA. Generation of multiple earthquake accelerograms compatible with spectrum via wavelet packet transform and stochastic

neural networks. *J Earthquake Eng*, 2009; **13**: 899-915.
7. Ghodrati Amiri G, Shahjouei A, Saadat S, Ajallooeian M. Hybrid evolutionary-neural network approach in generation of artificial accelerograms using principal component analysis and wavelet-packet transform. *J Earthquake Eng*, 2011; **15**: 50-76.
8. Dorigo M. *Optimization, Learning and Natural Algorithms* [in Italian]. PhD thesis, Dipartimento di Elettronica, Politecnico di Milano, Milan, 1992.
9. Mullen RJ, Monekosso D, Barman S, Remagnino P. A review of ant algorithms. *Expert Syst Appl*, 2009; **36**: 9608–17.
10. Dorigo M, Thomas S. *Ant Colony Optimization*. A Bradford Book, The MIT Press Cambridge, Massachusetts, London, England, 2004.
11. Dorigo M and Blum C. Ant colony optimization theory: A survey. *Theor Comput Sci*, 2005; **344**: 243-78.
12. Erdem H. Prediction of the moment capacity of reinforced concrete slabs in fire using artificial neural networks. *Adv Eng Softw*, 2010; **41**: 270-6.
13. Khashei M, Bijari M. An artificial neural network (p,d,q) model for time series forecasting. *Expert Syst Appl*, 2010; **37**: 479-89.
14. Xuefeng Y. Hybrid artificial neural network based on BP-PLSR and its application in development of soft sensors. *Chemo Intell Lab Syst*, 2010; **103**: 152-9.
15. Ocaka H, Loparo KA, Discenzo FM. Online tracking of bearing wear using wavelet packet decomposition and probabilistic modeling: A method for bearing prognostics. *J Sound Vib*, 2007; **302**: 951–61.
16. Fan XF, Zuo MJ. Gearbox fault detection using Hilbert and wavelet packet transform. *Mecha Syst Signal Process*, 2006; **20**: 966–82.
17. Ogden RT. *Essential Wavelets for Data Analysis*, Birkhäuser Boston, 1997.
18. Jolliffe IT. *Principal Component Analysis*, Springer Series in Statistics, 2nd edition, New York, 2002.
19. Conlanc XA, Bellomarino SA, Parker RM, Barnett NW, Adams MJ. Partial least squares and principal components analysis of wine vintage by high performance liquid chromatography with chemiluminescence detection. *Analyt Chim Acta*, 2010; **678**(1): 34–8.
20. Lu Wei-Zhen, He Hong-Di, Dong Li-yun. Performance assessment of air quality monitoring networks using principal component analysis and cluster analysis. *Build Environment*, 2011; **46**(3): 577-83.
21. Young FW, Takane Y, Leeuw JD. The principal components of mixed measurement level multivariable data: An alternating least squares method. *Psychometrika*, 1978; **43**(2): 279-81.
22. Naeim F. *The Seismic Design Handbook*, Kluwer Academic Publishers, 2nd Edition, Boston, MA, USA, 2001.
23. Chopra AK. *Dynamics of Structures: Theory and Application to Earthquake*. Prentice-Hall Inc, USA, 1995.
24. Gao W. New neural network based on ant colony algorithm for financial data forecasting. *Proceedings of the fourth International Conference on Intelligent Information Hiding and Multimedia Signal Processing*, China, 2008, pp.1437-1440.
25. Tehrani R, Khodayar F. Optimization of the artificial neural networks using ant colony algorithm to predict the variation of stock price index. *J Appl Sci*, 2010; **10**(3): 221-5.

26. Chengzhi C, Yifan W, Lichao J, Yang L. Research on optimization of speed identification based on ACO-BP neural network and application. *Proceedings of the Seventh World Congress on Intelligent Control and Automation*, Chongqing, China, 2008, pp. 6973-6977.
27. *MATLAB* Reference Guide, the Math Works Inc, 2004.
28. Riedmiller M, Braun H. A direct adaptive method for faster backpropagation learning: the RPROP algorithm. *Proceedings of the IEEE International Conference on Neural Networks* (ICNN), San Francisco, 1993, pp. 586–591.
29. Mukherjee S, Gupta VK. Wavelet-based generation of spectrum-compatible time-histories. *Soil Dynam Earthquake Eng*, 2002; **22**(9–12): 799–804.
30. Mukherjee S, Gupta VK. Wavelet-based characterization of design ground motions. *Earthquake Eng Struct Dynam*, 2002, **31**(5): 1173-90.
31. Ramezi H. *Base Accelerogram Data of Iranian Accelerograph Network*. Building and Housing Research Center, BHRC-PN S 253, Tehran, Iran, 1997.
32. Liu YP, Wu MG, Qian JX. Evolving neural networks using the hybrid of ant colony optimization and BP algorithms. *LNCS Springer-Verlag*, Berlin Heidelberg, 2006; **3971**: 714–22.
33. Newmark NM, Hall WJ. *Earthquake Spectra and Design*. Monograph published by Earthquake Engineering Research Institute, 1986.
34. Fugal DL. *Conceptual Wavelets in Digital Signal Processing*. Space & Signals Technologies LLC, 2009.